A combination of relative-numerical dating methods indicates two high Alpine rock glacier activity phases after the glacier advance of the Younger Dryas

Böhlert, R ; Compeer, M ; Egli, M ; Brandova, D ; Maisch, M ; Kubik, P W ; Haeberli, W

Abstract: To exploit the potential of rock glaciers as indicators of past climate condition it is first necessary to date them. The combined application of both relative and absolute dating techniques is a promising approach. In this study, we present Schmidt-hammer rebound value measurements and weathering rind thicknesses on four active and one relict rock glacier in the Albula area of the eastern Swiss Alps. Associated landforms such as the moraines in front of rock glaciers and glacially polished bedrock also were used to set up the temporal framework. This was done using soil chemical analyses, radiocarbon dating of the stable fraction of soil organic matter and surface exposure dating of boulders. Schmidt-hammer and weathering rind measurements showed, in most cases, well-pronounced trends with increasing surface ages. These values are in line with measurements from other nearby rock glaciers with comparable lithologies. Use of this information together with the numeric ages makes it possible to derive two main activity phases: one started soon after the ice retreat following the Younger Dryas, the main activity occurred most likely in the early Holocene and lasted approximately until the Holocene climate optimum. The second activity phase continues today and had an unclear start between 10 to 6 cal ky BP.

DOI: https://doi.org/10.2174/1874923201104010115

A Combination of Relative-Numerical Dating Methods Indicates Two High Alpine Rock Glacier Activity Phases After the Glacier Advance of the Younger Dryas

Ralph Böhlert[1], Michael Compeer[1], Markus Egli[*,1], Dagmar Brandová[1], Max Maisch[1], Peter W. Kubik[2], Wilfried Haeberli[1]

[1]*Department of Geography, University of Zurich, CH-8057 Zurich, Switzerland*

[2]*Institute of Ion Beam Physics, ETH-Hönggerberg, CH-8093 Zurich, Switzerland*

Abstract: To exploit the potential of rock glaciers as indicators of past climate condition it is first necessary to date them. The combined application of both relative and absolute dating techniques is a promising approach. In this study, we present Schmidt-hammer rebound value measurements and weathering rind thicknesses on four active and one relict rock glacier in the Albula area of the eastern Swiss Alps. Associated landforms such as the moraines in front of rock glaciers and glacially polished bedrock also were used to set up the temporal framework. This was done using soil chemical analyses, radiocarbon dating of the stable fraction of soil organic matter and surface exposure dating of boulders. Schmidt-hammer and weathering rind measurements showed, in most cases, well-pronounced trends with increasing surface ages. These values are in line with measurements from other nearby rock glaciers with comparable lithologies. Use of this information together with the numeric ages makes it possible to derive two main activity phases: one started soon after the ice retreat following the Younger Dryas, the main activity occurred most likely in the early Holocene and lasted approximately until the Holocene climate optimum. The second activity phase continues today and had an unclear start between 10 to 6 cal ky BP.

Keywords: Rock glaciers, relative and numerical dating techniques, soils, moraines.

INTRODUCTION

Rock glaciers as distinct tongue-shaped landforms are perennially frozen and ice-rich debris on non-glacierised mountain slopes creeps steadily under the influence of gravity [1]. Active rock glaciers (i.e., they contain ice and deform) are supposed to have formed and evolved during the Holocene and can be seen as transport systems. They may bear long-term palaeoclimatic information [2]. Relict forms on lower altitudes have lost their ice content and do not creep anymore. As they initially must have formed under permafrost conditions as well, they have a considerable potential for constraining former climatic conditions [3]. Thus, dating of such landforms is relevant for any kind of paleoclimatic reconstructions and interpretation.

With time, the surface of rock glaciers is increasingly subject to weathering processes. Usually, the older the surface of rock debris the more pronounced is the imprint of weathering. Relative and numeric age dating by measuring the weathering rind thickness or the Schmidt-hammer rebound value was successfully performed on moraines and rock glaciers developed on sandstones in New Zealand [4-8], basaltic and andesitic boulders in North America and Japan [9, 10] and on granites and gneiss in the Alps [2, 11]. Weathering rinds have also a certain potential for numeric dating using isotopes [12].

*Address correspondence to this author at the Department of Geography, University of Zurich, CH-8057 Zurich, Switzerland; Tel: +41 (0)44 635 51 14/21; Fax: +41 (0)44 635 68 41; E-mail: markus.egli@geo.uzh.ch

During the past decades, several studies have been carried out to determine the age of rock glaciers in the European Alps [13-15]. Kääb *et al*. [16] used photogrammetric methods to obtain flow trajectories and to estimate ages of rockglacier surfaces. Haeberli *et al*. [17] proposed a multiple approach using relative and numerical dating to obtain more conclusive information on rock-glaciers dynamics. A 'cross-check' of these methods allows an extended interpretation and reciprocal control of the results. Such an approach has until now rarely been done for Alpine geomorphic features. The scope of the present paper is, therefore, to test and apply several dating techniques for assessing the age and activity phases of several rock glaciers in a high Alpine region of the Swiss Alps.

STUDY AREA

The study area is located in the eastern Swiss Alps (Fig. **1**). The area of the Albula pass is characterised by many glacial and geomorphic features such as moraines, polished bedrock with roches moutonnées, scree slopes, rock glaciers, traces of glacial erosion (such as grooves, striations, etc.) and plucking processes. Tectonically, the region southern of the Albula pass is situated within the Err-Bernina nap that belongs to the lower Austroalpine. The greenish 'Albula Granite' is the dominant rock type [18-20]. The adjacent area to the north of the Albula pass belongs to the Ela nap, composed mainly of sedimentary rock types and denotes a sharp contrast to the Err-Benina nap. The mean annual precipitation is rather low with around 900 mm in the lower parts near Preda and up to 1100 mm towards the mountain

1874-9232/10

ridges [21]. The reconstructed Last Glacial Maximum (LGM) ice surface geometry based on glacial-geological mapping shows that the area was situated near the 'Engadine' ice dome culminating in the Upper Engadine [22, 23]. Trimline and other erosional features indicate that during LGM the Albula pass formed a transfluence with ice flowing from the Engadine into the Rhine river system [24]. The Lateglacial footprint (moraine sequence) north to the ridge Piz da las Blais – Crasta Mora (Fig. **1**) was formed as a result of a slope-glaciation [25]: only at the western boundary of the former glacier did a distinct ice-tongue develop, as indicated by moraines. This former tongue area is today occupied by the relatively long rock glacier Alvra (rock glacier E, Fig. **1**). Except for the two cirques to the NW and NE of Crasta Mora, there are no signs for the existence of glacier ice during the Little Ice Age [25, 26]. Fig. (**2**) gives an overview of the calculated modern permafrost distribution [27]. The position of the rock glaciers A – D in the north exposed slopes (see also Fig. **3**) is clearly identifiable within the continuous permafrost. In the area of the rock glacier E only some sporadic permafrost can be expected.

Five rock glaciers near the Albula pass were investigated (for details, see Figs. **3-5**). Four are still active, as indicated by the lack of vegetation, (A – D; Figs. **3**, **4**) whereas the rock glacier Alvra (E) is relict. The rock glacier Alvra lies at a lower altitude than the others (Fig. **5**) and lies between 2040 and 2320 m asl with a west orientation. All other rock glaciers are at an altitude of about 2400 up to 2700 m asl and have north-facing exposures. While the active rock glaciers show a simple structure with a clearly identifiable rooting zone and a compact steep tongue, the conditions in case of the rock glacier Alvra are more complex. Geometry (long shape) and a rather flat slope in the middle and upper part (Fig. **5**) suggest a debris supply from several steep debris sources within the slopes that are unified in the rock glacier Alvra (indicated by arrows in Fig. **5**). Consequently, along the flow line of the rock glacier Alvra, several small rock glaciers are crossed and hence a well-developed age trend cannot be expected. In addition to the investigations on rock glaciers, two soil profiles were studied (Fig. **6**). One of them is on a moraine assigned to the Egesen glacial state [25] and close to the relict rock glacier (site: "Igls Plans") and the other one directly below an active rock glacier (site: "Peidra Mora"). In addition, two samples for surface exposure dating from a roche moutonnée (site "Crap Alv") were analysed to derive a maximum age for deglaciation (which must have preceded rock glacier formation) close to the rock glacier tongue and consequently for the start of rock glacier activity. In close vicinity, previously-reported data of a peat bog was available [25].

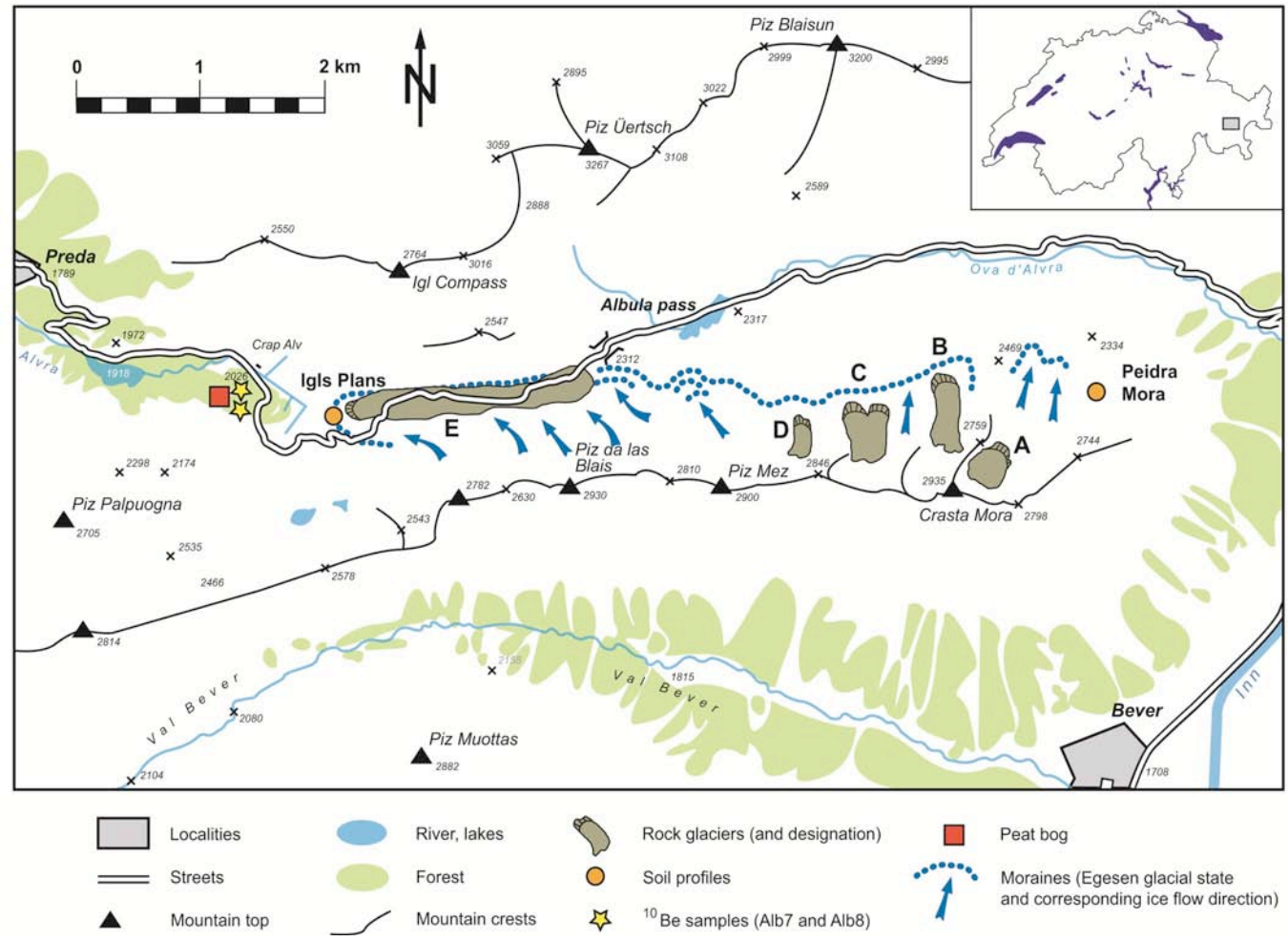

Fig. (1). Location of the investigation site.

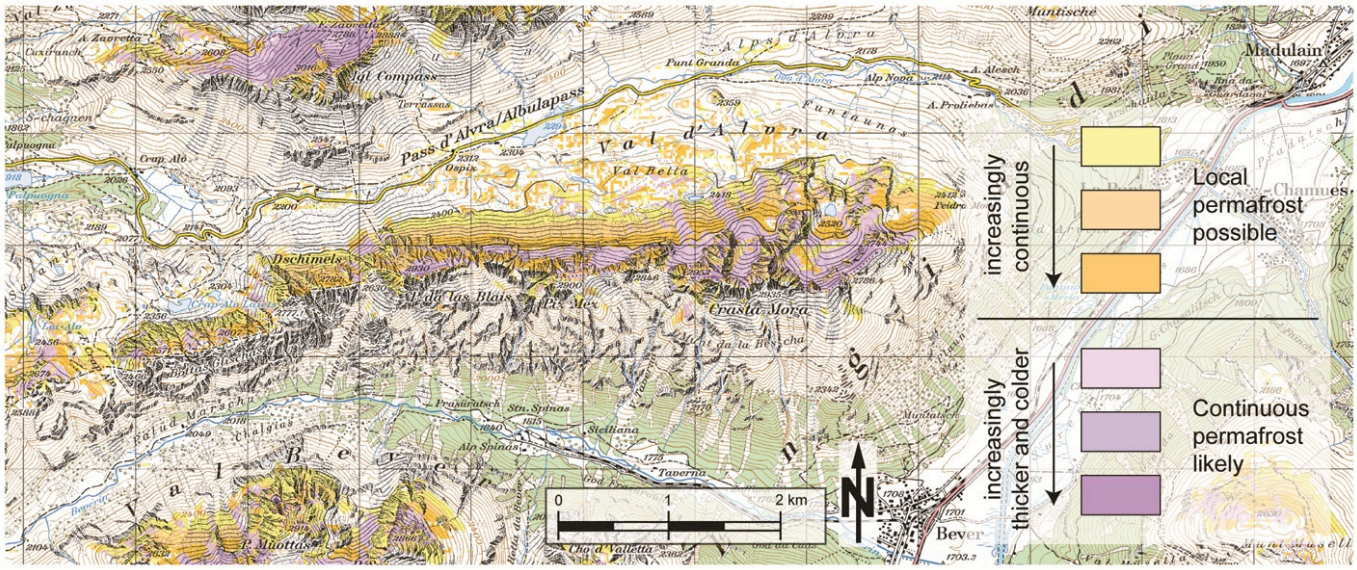

Fig. (2). Spatial distribution of local (sporadic) and continuous permafrost in the investigation area (data source: [27]).

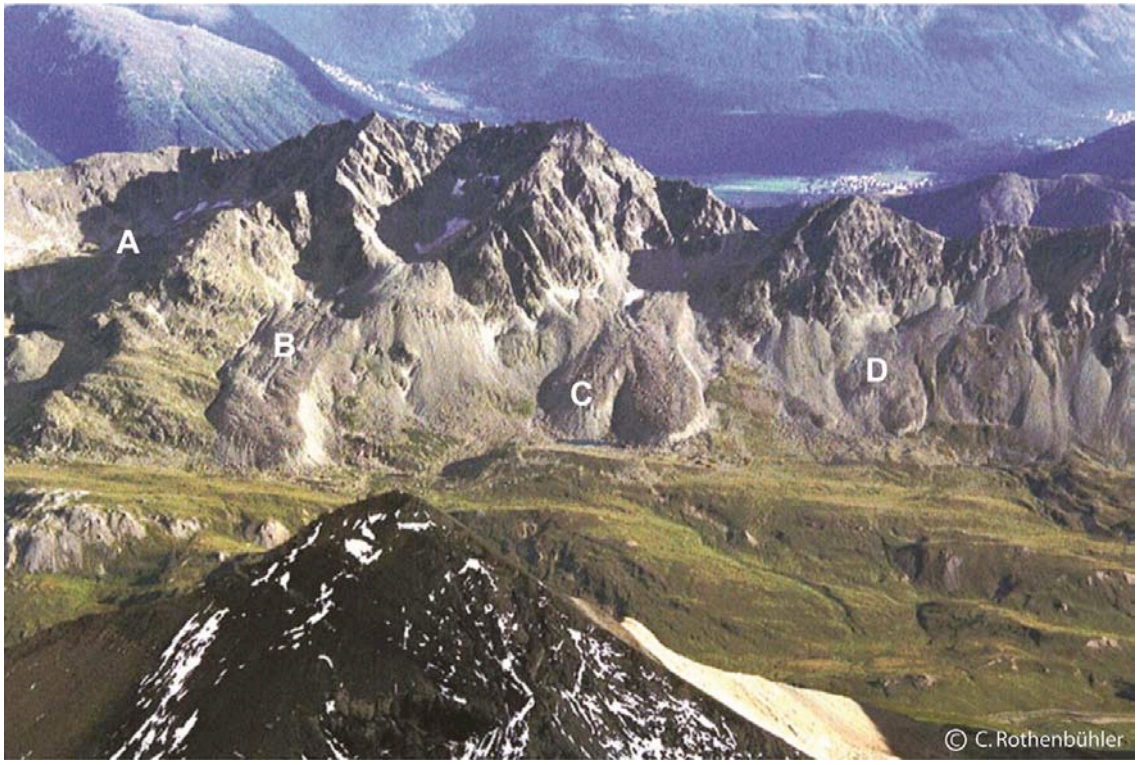

Fig. (3). Aerial photo (with a view in southern direction) of the investigated rock glaciers **A-D**.

MATERIALS AND METHODS

Schmidt-Hammer Rebound Values

The Schmidt-hammer is a portable instrument originally developed to test concrete quality in a non-destructive way [28]. A spring-loaded bolt impacting a surface yields a rebound- or R-value, which is proportional to the hardness (compressive strength) of a rock surface. Applied in geomorphology, old rock surfaces exposed to weathering processes for a long time provide low R-values and vice versa. Since the 1980s the method has also been successfully used for relative age dating of gemorphologic features such as moraines [14, 29, 30], rock glaciers ([2, 31] or rockfall deposits [32]. Recent publications increasingly discuss the possibilities and limitations to calibrate R-values, for instance with results from ^{10}Be and ^{14}C-analyses [33, 34] or optically stimulated luminescence and photogrammetrical measurements [2, 17].

In this study the N-type Schmidt-Hammer (Proceq, Switzerland) was used. On each mapped unit (e.g. moraine, rock glacier lobe) 50 randomly selected boulders/sites were measured, avoiding edges of boulders [35], spots that

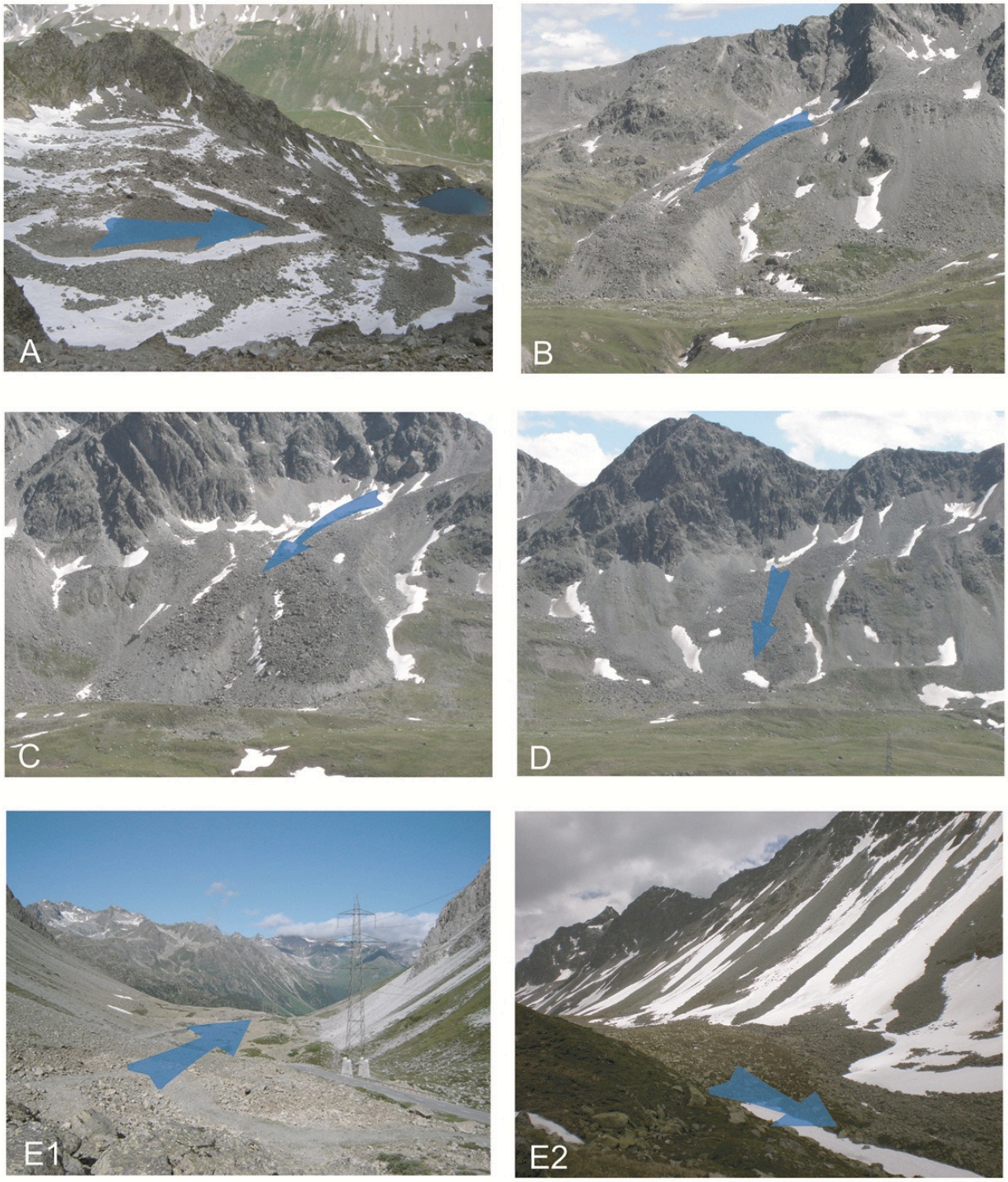

Fig. (4). Detailed view of the investigated rock glaciers **A-D**. The uppermost part of the relict rock is shown in E1 and the middle and lower part in E2.

showed lichen growth as well as visual fissures or cracks. Only flat parts under dry conditions were considered. The hardness of an analysed form is represented by the arithmetic mean of the individual records. Following the suggestions by [30], we used a standard error based on the standard deviation in a 95% confidence interval to get statistically significant hardness variations and by extensions age differences:

$$x \pm 1.96 \times \sqrt{\left(\sigma / \sqrt{n}\right)} \quad (1)$$

where x is the arithmetic mean, σ the standard deviation and n corresponds to the number of measurements.

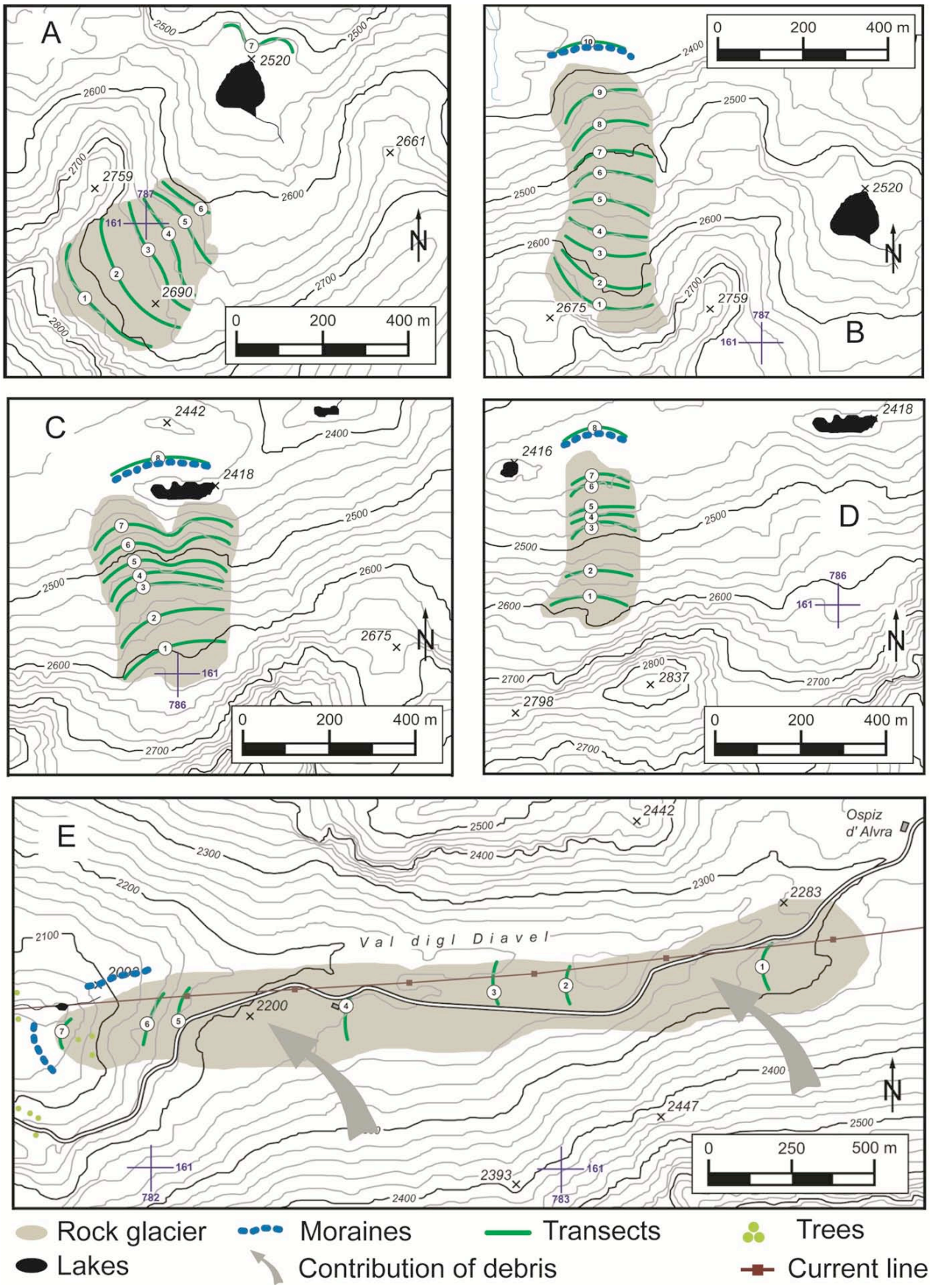

Fig. (5). Detailed topographic sketch of the investigated rock glaciers with sampling transects (Schmidt-hammer; and in close vicinity weathering rinds).

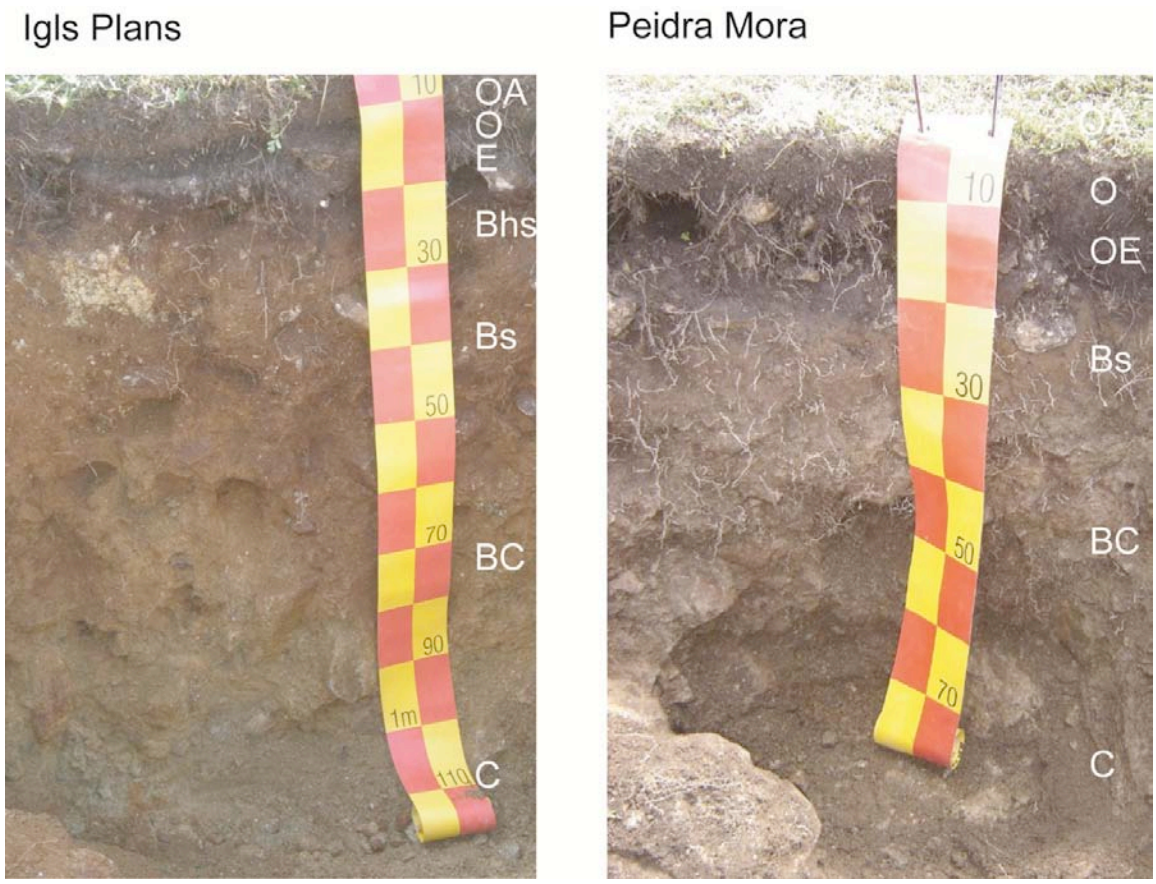

Fig. (6). Profile photos and horizon designations of the investigated soils (see also Fig. **1**).

Weathering Rind Thicknesses

Rock surfaces exposed to the atmosphere are subject to (biogeo-)chemical weathering processes that result in a coloured outer crust around the rock. For commonly used definitions and involved processes see [36] and references therein. The time dependent rind growth towards the rock-center is used as an indicator of relative ages of glacial and periglacial deposits. A great number of investigations has been carried out mainly on Holocene moraines and fluvial terraces with different lithologies in Western USA, New Zealand and Japan [e.g. 4, 8, 9]. An extensive overview of previous studies on weathering rinds since the 1960s is given in [36]. Limitations and potential error sources such as erosion are discussed thoroughly in [37].

At each site (top of moraines and rock glacier lobes) 50 rind-samples were chipped with a hammer from boulders with a minimum diameter of approx. 30-40 cm. The weathering rind was measured perpendicular to the surface with a 0.1 mm scale graduated magnifying glass. Edges and cracks leading to larger rind thicknesses and an overestimation of weathering stages were avoided. Also rock pieces were omitted that showed inside weathering traces indicating a pre-failure. In the following, the mean, the median and the modus value are given as relative age indicators.

Soil Chemistry and Physics

The soil samples were air-dried, large aggregates were gently broken by hand and sieved to <2 mm. Total C and N contents of the soil were measured with a C/H/N analyser (Elementar Vario EL, Elementar Analysensysteme GmbH) using oven-dried and ball-milled fine earth. Total C corresponds in our case to organic C due to the absence of any carbonates in the soil (granite till as parent material and very low pH values in the soil horizons). Soil pH (in 0.01 M $CaCl_2$) was determined on air-dried samples of the fine earth fraction using a soil solution ratio of 1:2.5.

Element pools in the soil (Fe, Al, Si, Ti) were determined by a total dissolution method. Oven-dried samples were dissolved using a mixture of HF, HCl, HNO_3, and H_3BO_3 in a closed system [38] (microwave oven and under high pressure, 25 bar). Concentrations were determined by AAS (Atomic Absorption Spectrometry – AAnalyst 700, Perkin Elmer, USA). The dithionite- and oxalate-extractable fractions were measured for the elements Fe, Al and Si [39].

After a pre-treatment of the samples with H_2O_2 (3%) on heat, the particle size distribution of the soils was measured by a combined method consisting of sieving the coarser particles (2000 - 32 µm; [40]) and the measurement of the finer particles (< 32 µm) by means of an X-ray sedimentometer (SediGraph 5100).

Fractionation of Organic Matter

Acting on the assumption that chemical oxidation mimics natural oxidative processes, we treated the soils with 10% H_2O_2 to eliminate the more labile organic material from the more refractory organic matter [41-44]. The stable fraction that remained at the end of the treatment can comprise the

first organic matter formed in the sediment after glacier retreat [45] and may, under certain circumstances, provide a minimum age of deposition of the moraines and of deglaciation. One gram of air-dried soil was wetted for 10 min with few ml of distilled water in a 150 ml beaker. Afterwards, 90 ml of 10% H_2O_2 were added. The procedure was run at a minimum temperature of 50°C throughout the treatment period. The beakers were closed with two layers of parafilm to avoid evaporation of the reagent. H_2O_2 treatments were performed for 168 hours (7 days). At the end of the treatment the samples were washed three times with 40 ml deionised water, freeze-dried, weighed, analysed for total C and N and ^{14}C dated.

Radiocarbon Dating

The CO_2 of the combusted samples was catalytically reduced over iron powder at 550°C to elemental carbon (graphite). The obtained mixture was pressed into a target and the ratios ^{14}C:^{12}C (for radiocarbon age) were measured by Accelerator Mass Spectrometry (AMS) using the tandem accelerator of the Institute of Particle Physics at the Swiss Federal Institute of Technology Zürich (ETHZ). The calendar ages were calculated with the OxCal 4.1 calibration program [46] based on the IntCal 04 calibration curve [47]. Calibrated ages are given in the 2 σ range (minimum and maximum value).

Cosmogenic Dating

The cosmogenic nuclide concentrations (e.g. ^{10}Be) in the surface of moraine boulders and polished bedrock exposure reflect the time that has passed since the moraine stabilised [48] and the ice retreated and exposed the landform to cosmic ray flux.

Rock samples were removed with hammer and chisel and split apart. Only the uppermost $\leq$ 5 cm of the rock surfaces was used for dating. Because of possible edge effects [49], marginal positions on sharply shaped boulders were avoided. The rock samples were crushed, sieved and leached in order to obtain pure quartz following [50, 51]. $^{9}Be(NO_3)_2$ solution was added as a carrier to the dried quartz which was then dissolved in 40% HF. The Be was isolated using anion and cation exchange columns followed by selective pH $Be(OH)_2$ precipitation [51]. The Beryllium hydroxide was calcinated to BeO and than pressed into an AMS target. The $^{10}Be/^{9}Be$ ratios were measured by AMS using the tandem accelerator facility at the Swiss Federal Institute of Technology Zurich (ETHZ) using ETH AMS standard S555 ($^{10}Be/^{9}Be = 95.5 \times 10^{-12}$ nominal) with a ^{10}Be half-life of 1.51 Ma. The surface exposure ages were calculated using a sea-level high-latitude production rate of 5.1 ± 0.3 ^{10}Be atoms/g SiO_2/year with a 2.2 % production due to muon capture [52]. Production-rate scaling for latitude (geographic) and altitude was based on [52] and corrected for sample thickness assuming an exponential depth profile, a rock density of 2.65 g cm^{-3} and an effective radiation attenuation length of 155 g/cm^2 [48]. Topographic shielding was based on a zenith angle dependence of $(\sin\theta)^{2.3}$ [53]. Topographical shielding was calculated using a 25 m DEM (Digital Elevation Model - source: swisstopo) and a geographical information system (ArcGIS 9.2). The production rate was corrected for mean snow cover. The snow cover height was estimated for the period November - April based on measurements from 1983-2002 made at three nearby weather stations (data source: Swiss Federal Institute for Snow and Avalanche Research, MeteoSwiss). A mean snow height of 1.5 m during six months could be derived and seems to be a realistic value for 2500 m asl in this region. The theoretical snow height for the sample site was estimated using a mean snow height gradient of 0.08 m/100 m altitude difference [54]. Factors such as boulder shape, wind exposition and vegetation led to additional corrections whereas the highest reductions in snow height were caused by steeply dipping boulders. In addition, satellite images taken in June from three different years (Spot images, 1993-1995), were compared in regard to the snow cover in the investigation area. The geomagnetic field correction was omitted because its effect is insignificant in comparison to the other corrections.

RESULTS

Weathering rind Thicknesses

The weathering rinds were generally very thin (Fig. **7**). Nonetheless, the median and mean values showed a clear increase from the youngest part near the rockwall to the frontal talus of the rock glacier (Fig. **7A-E**). Thicknesses of weathering rinds increased towards the distal front of the rock glaciers. Near the cirque headwalls, the weathering rind thickness was close to 0 mm and increased to 1.5 mm at the front of the rock glacier. The rock glacier Alvra (E) had, according to the expectance, the highest values with about 1.0 mm near the headwall and about 2.0 mm at the snout.

The literature indicates that the modal values should be used to delineate trends along a rock glacier. Generally, the trend obtained with the modal values follows approximately those of the mean and median values. The time dependent tendency looked, however, more disturbed.

The weathering rinds of the roche moutonnée and the frontal moraines are near 1.5 and 2.0 mm. The frontal moraines were supposed to be from a Younger Dryas glacier advance (Egesen glacial state; [25]). The observed sequence of weathering rind growth corresponds with the geomorphologic settings and, therefore, seems to be an appropriate tool for reconstructing the relative age sequences here.

Schmidt-Hammer Rebound Values

The measured Schmidt-hammer rebound values for all rock glaciers are given in Fig. (**8A-D**). We observed distinct trends along the rock glaciers, with lower values at the distal fronts. The standard error after [30] was in most cases relatively small. Rock glacier A shows that many blocks were turned over close to the distal front and, consequently, gave higher rebound values (which would indicate a younger age). The present-day active rock glaciers showed at their front Schmidt-hammer rebound values near 40. Close to the cirque, the values were usually near 50-55. An exception is the inactive, relict rock glacier Alvra (E). At the distal front, the rebound values were near 30 but at the start the values were near 40. The tongues of most of the rock glaciers lie inside (upvalley from) frontal moraines (Younger Dryas [25]) or a roche moutonnée that became ice-free after the Egesen glacial state. The rebound values for these features were in the range of 30-35 and therefore close to the values measured at the front of rock glacier Alvra. This suggests

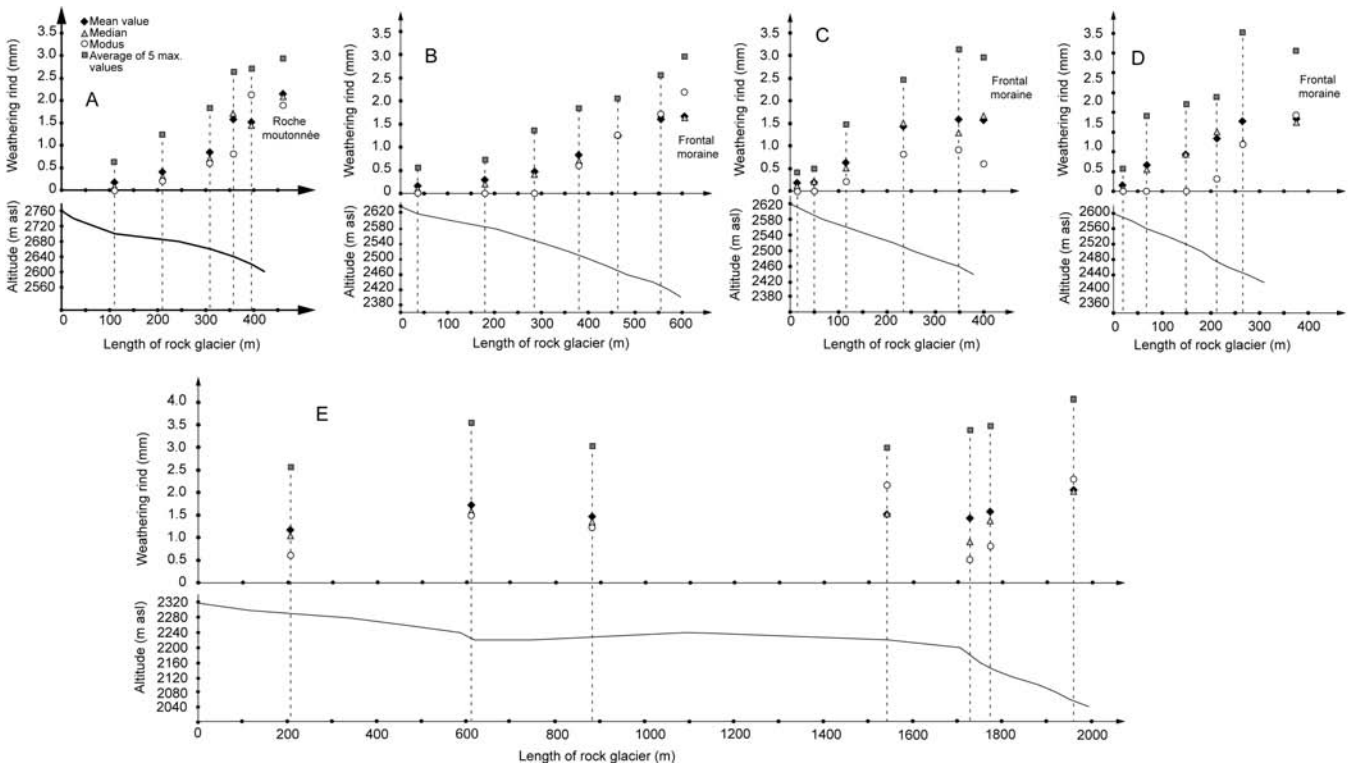

Fig. (7). Weathering rind thickness (average, median, modus and average of the 5 max. values) along the investigated rock glaciers. For the sites **A-D**, a comparison was possible with a frontal moraine or a roche moutonnée (in the case of A) close to the front of the rock glacier.

that the activity of rock glacier Alvra began soon after the retreat of the Egesen-age glaciers. All other rock glaciers started their activity later. The measured Schmidt-hammer values at the distal front of these rock glaciers correspond approximately to the initial values of rock glacier Alvra (near 40-45).

Soils and Weathering Losses

The physical and chemical characteristics of the soils are given in Tables **1** and **2**. The profile Igls Plans developed on a frontal moraine and the profile Peidra Mora on glacial till (ground moraine). Both profiles are in the vicinity of rock glaciers. The soil profiles have loam or sandy-loam textures in the topsoil and a loamy-sand texture in the subsoil (Table **1**). The soils are decidedly acid with pH-values in the topsoil < 4 (Table **2**). In both soils, weak to strong podzolisation is recognised as indicated by the translocation of Fe, Al and, especially at the site Igls Plans, organic C. In both soils, the translocation of Fe within the soil profile is evident. The Fe_o/Fe_d ratio in the topsoil of both sites is similar. A higher Fe_o/Fe_d ratio in the Bhs and Bs horizon (with values of 73 and 61%, respectively) and also higher concentrations of both Fe_o and Fe_d were measured at the site Igls Plans. The parameter $Al_o + 0.5Fe_o$ (Table **2**) clearly reflects the spodic characteristics of the soil at Igls Plans (see [55]). Furthermore, organic C is translocated to greater depths at the site Igls Plans than at the site Peidra Mora where such a translocation is much less obvious or even absent. This clearly indicates that the podzolisation features are more pronounced at the site Igls Plans. Some imogolite-type materials were detected in the profile "Igls Plans" (indicated by the oxalate-extractable Si). In general, the soil profile "Igls Plans" was better developed and consequently, it has undergone a longer duration of soil development.

Long-term weathering rates of soils were derived using immobile element contents [56-58]. Ti was used as an immobile element. The parameter $\tau_{j,w}$ represents the open-system mass transport function and is defined as [57]:

$$\tau_{j,w} = \frac{C_{j,w}C_{i,p}}{C_{j,p}C_{i,w}} - 1 \qquad (2)$$

where $C_{j,p}$ (kg/t) is the concentration of element j in protolith (e.g., unweathered parent material, bedrock), $C_{j,w}$ is the concentration of element j in the weathered product (kg/t), $C_{i,p}$ (kg/t) the concentration of the immobile element i in the protolith (e.g., unweathered parent material, bedrock) and $C_{i,w}$ the concentration of the immobile element i in the weathered product (kg/t).

Chemical concentration profiles in soils and regoliths can identify five end-member categories of elemental profiles [59]: (1) immobile profiles exhibit parent concentrations at all depths; (2) depletion profiles exhibit losses at the top, grading to parent concentration at depth; (3) depletion-enrichment profiles exhibit depletion at the top, enrichment at depth resulting from precipitation or translocation, and a return to parent concentration at greater depth; (4) addition profiles show enrichment from external input at the top grading to parent concentration at depth; and (5) biogenic profiles exhibit enrichment at the top and a depleted zone that grades downward to parent concentration at depth.

In the analysed soils, Fe is strongly leached at the surface (Fig. **9**) and translocated to depth resulting in a typical

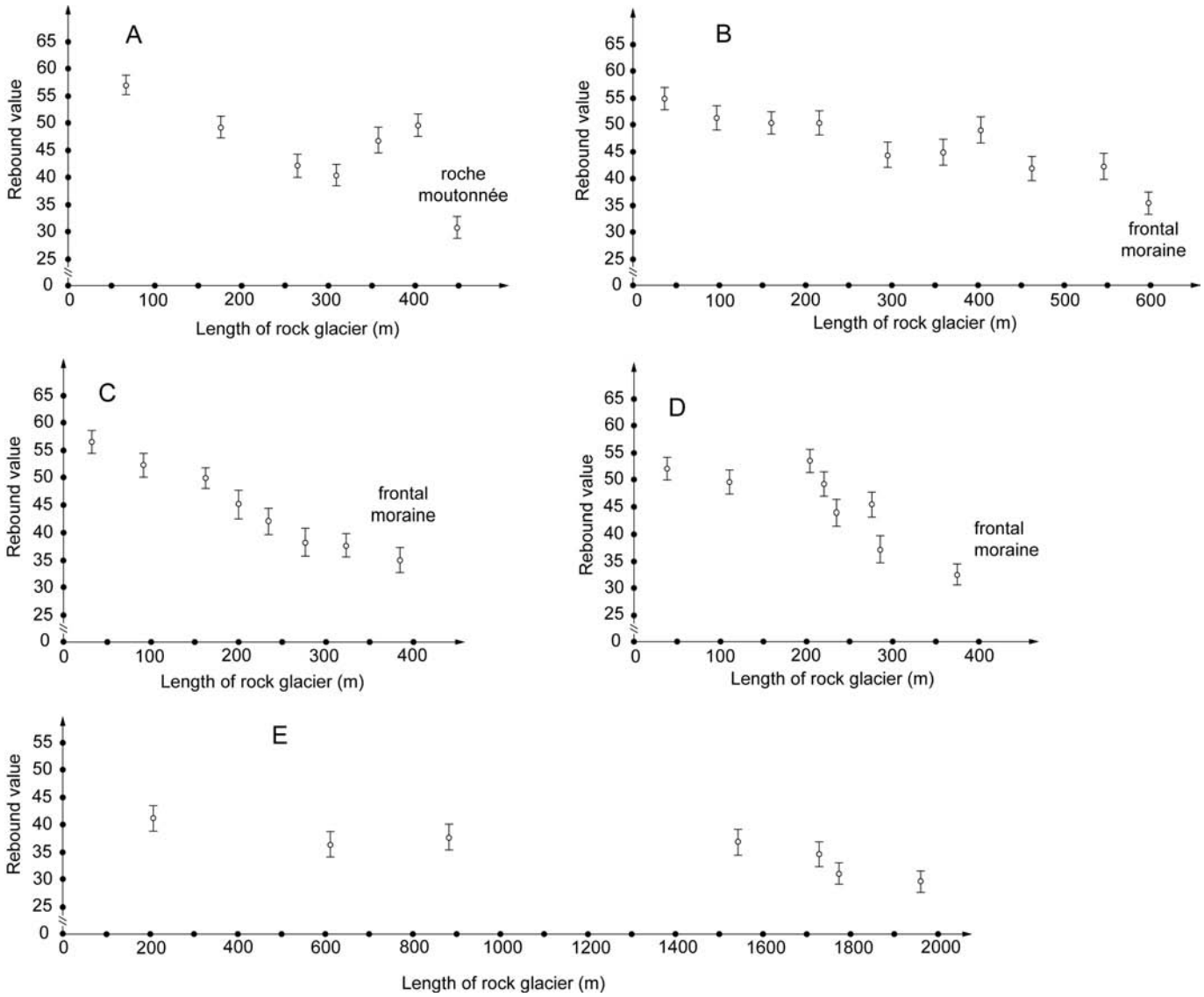

Fig. (8). Schmidt-hammer rebound values and standard error according to [28] along the investigated rock glaciers. For the sites **A**, **B**, a comparison was possible with a frontal moraine or a roche moutonnée, each representing a Lateglacial reference, close to the front of the rock glacier.

depletion-enrichment profile (type 3). Al and Si show a strong depletion in the topsoil and a weak enrichment in the subsoil. Consequently, the two elements are at the transition between a depletion profile (type 2) and a depletion-enrichment profile (type 3). Weathering losses were generally higher (lower τ value; Fig. **9**) at the site "Igls Plans". Very intense leaching of the elements Fe or Al was measured in the O and E horizon. Mass transfer functions indicated losses of up to 80%. In the Bs and BC horizon, a substantial part of the leached Al and Fe was reprecipitated. Weathering and the eluviation and illuviation (due to podzolisation) of Fe and Al were in general more pronounced at "Igls Plans" (Table **2**; Figs. **6**, **9**) than at "Peidra Mora". Also the resulting concentration of oxyhydroxides (Fig. **10**) was higher at the site "Igls Plans". The weathering status of the soil "Igls Plans" is typical for Alpine soils which have developed over the entire post-Egesan period [60, 61].

Surface Exposure and ^{14}C Dating

The samples of the roche moutonnée Crap Alv (Alb7 and Alb8) gave nuclide exposure ages of 12.5 ± 0.9 and 11.8 ± 1.5 ky respectively. This suggests that this polished bedrock site must have become ice-free at the beginning of, or at the latest, within the Younger Dryas (Table **3**). This age estimate is in agreement with ages from a nearby peat bog where an age range of 10246 – 11090 cal BP was obtained (minimum age).

In contrast, palynological investigations of the deepest inorganic layer of this peat bog suggest a pre-Allerød age (Allerød: 14.7 – 12.9 ky BP) of ice recession (Burga in: [25]). This interpretation is supported by geomorphologic mapping, which shows that this locality can be interpreted as a part of the intramoraine area of the Daun stadial glaciation [25]. At present, we do not have a plausible explanation for these differences in the timing of deglaciation. Factors such as underestimated values for erosion, snow or sediment

Table 1. Physical Characteristics of the Soil Profiles

Site	Horizon	Depth (cm)	Munsell Colour (Moist)	Sand (%)	Silt (%)	Clay (%)	Bulk Density (g cm^{-3})	Skeleton (%)
Igls Plans	OA	0-10	7.5 YR 3/2	n.m	n. m.	n. m.	0.66	25.8
	O	10-15	7.5 YR 2/2	26.4	55.5	18.1	0.66	14.7
	E	15-20	10 YR 2/2	34.0	49.7	16.3	0.70	12.9
	Bhs	20-25	10 YR 2/2	36.8	54.4	8.8	0.76	39.8
	Bs	25-55	7.5 YR 3/4	54.8	36.2	9.0	0.88	62.7
	BC	55-105	7.5 YR 4/4	79.9	18.2	1.9	1.52	69.4
	C	> 105	10 YR 6/3	67.7	27.0	5.3	1.81	62.3
Peidra Mora	O	0-13	5 YR 1.7/1	n.m.	n. m.	n. m.	0.36	0.4
	OE	13-27	7.5 YR 2/2	18.2	68.4	13.4	0.84	44.3
	Bs	27-40	10 YR 3/3	28.9	45.7	25.3	1.11	37.3
	BC	40-70	10YR 4/3	74.0	22.7	3.3	1.66	82.0
	C	>70	10 YR 3/3	83.4	14.1	2.5	1.85	78.6

n.m. = not measured.

Table 2. Geochemical Characteristics of the Soil Profiles

Site	Horizon	pH ($CaCl_2$)	C (g kg^{-1})	N (g kg^{-1})	C/N	Fe_o* (g kg^{-1})	Fe_d** (g kg^{-1})	Al_o* (g kg^{-1})	Al_d** (g kg^{-1})	Si_o* (g kg^{-1})	$Al_o + 0.5Fe_o$ (%)	Fe_{Total} (g kg^{-1})	Al_{Total} (g kg^{-1})	Si_{Total} (g kg^{-1})	Ti_{Total} (g kg^{-1})
Igls Plans	OA	3.90	114.3	8.55	13.4	5.54	10.12	5.35	5.40	0.54	0.81	n. m.	n. m.	n. m.	n. m.
	O	3.80	112.1	7.74	14.5	3.06	5.63	3.49	3.62	0.37	0.50	52.8	53.1	267.0	6.51
	E	3.70	52.2	3.76	13.9	1.66	4.14	3.07	2.33	0.39	0.39	31.1	82.7	341.9	7.44
	Bhs	3.80	94.8	5.81	16.3	19.75	26.92	4.73	7.67	0.71	1.46	n. m.	n. m.	n. m.	n. m.
	Bs	4.15	46.6	1.94	24.0	12.57	20.68	11.20	12.54	1.09	1.75	192.0	82.8	286.7	6.44
	BC	4.70	15.1	0.64	23.5	3.42	8.98	8.26	6.33	2.19	1.00	145.2	81.7	323.4	4.32
	C	4.80	5.8	0.17	33.8	2.49	6.14	4.57	3.71	1.30	0.58	144.0	84.6	361.3	5.42
Peidra Mora	O	3.85	333.6	16.40	20.3	4.02	6.78	6.33	6.15	0.00	0.83	n. m.	n. m.	n. m.	n. m.
	OE	3.90	62.3	2.76	22.6	5.33	13.14	6.35	5.73	0.15	0.90	141.4	81.8	381.0	5.66
	Bs	4.00	19.3	0.97	19.8	5.38	13.32	3.74	4.48	0.49	0.64	174.5	82.2	344.6	7.26
	BC	4.30	8.6	0.22	39.0	0.88	4.28	1.82	2.20	0.25	0.23	108.4	78.2	387.7	4.52
	C	4.50	4.5	< 0.1	-	2.46	2.33	1.52	1.51	0.30	0.28	100.8	79.5	383.7	4.33

n.m. = not measured.
*o = oxalate-extractable amount.
**d = dithionite-extractable amount.

depth or vegetation coverage lead to exposure ages that are younger than the proposed stadial record. The fresh morphology of the bedrock surface gives no hint that a higher correction factor for erosion should have been chosen. For the same reason, sediment coverage during the earliest part of exposure can be excluded with a high degree of certainty. Since the roche moutonnée is situated below the timberline, it seems that an influence on age by vegetation in the past should, at least, be considered as possible, although its effect on the local ^{10}Be production rate is generally estimated to be rather low. In the case of trees and leaves a reduction of less than 4% would need to be taken into account [62]. Despite this uncertainty, we must assume that this area became ice-free about 12 ky to 15 ky (pre-Allerød) BP. The obtained numerical ages (which appear rather too young) and the palynological investigations are at least minimum-limiting ages and show that the rock glacier Alvra must be definitely younger. A maximum age for the rock glacier activity is the supposed Egesen glacial moraine (11.6 – 12.9 ky; [23]) in front of the rock glacier Alvra.

The age of the oldest organic matter fraction in the soil Peidra Mora is near 6 ky BP (Table **4**). In creeping permafrost, soil formation is inhibited or very much limited due to the continuous removal of the surface layers. Permafrost activity most probably has stopped c. 6 ky cal BP

ago which then gave rise to the start of soil formation. This soil is located at an altitude of 2400 m and lies between the present-day active rock glaciers and the start of the relict rock glacier Alvra. This gives another indication of the minimum age of the present-day active rock glaciers and an indication of when the rock glacier Alvra became inactive.

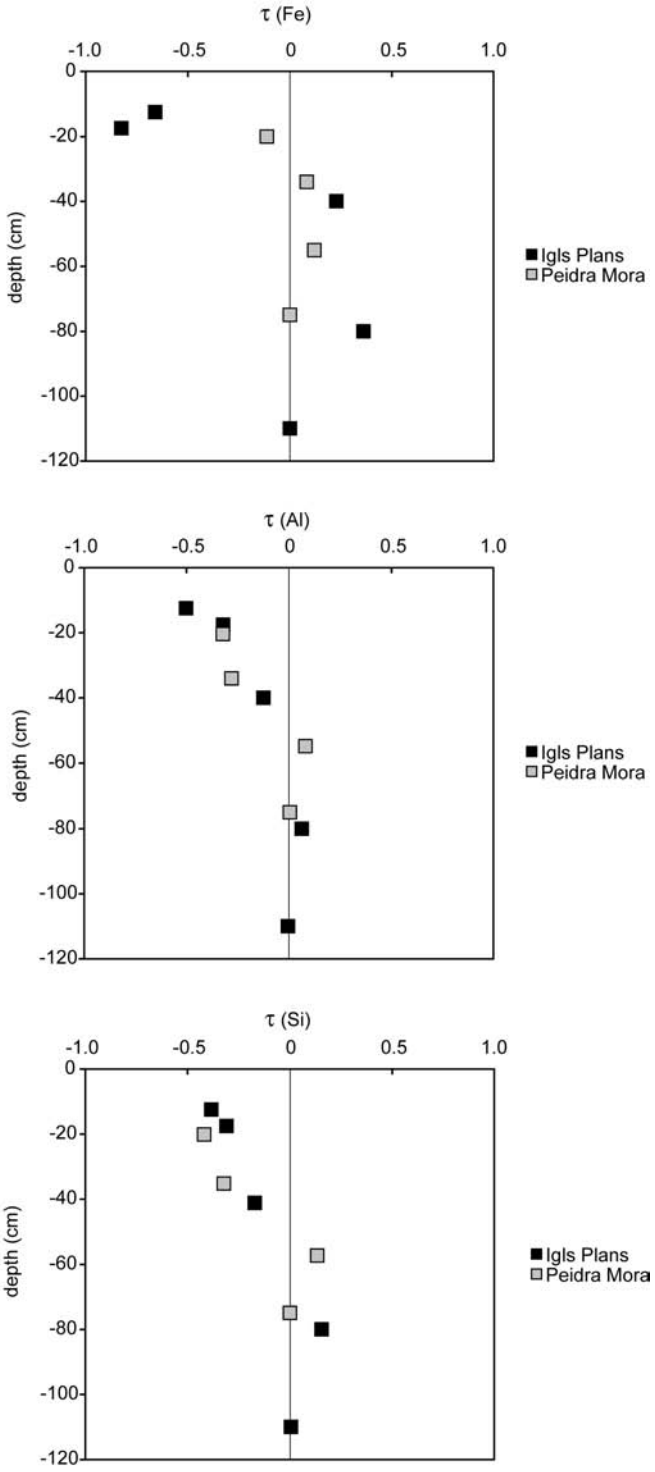

Fig. (9). Open system mass transport function $\tau_{j,w}$ for Fe, Al and Si as a function of soil depth of the investigated profiles.

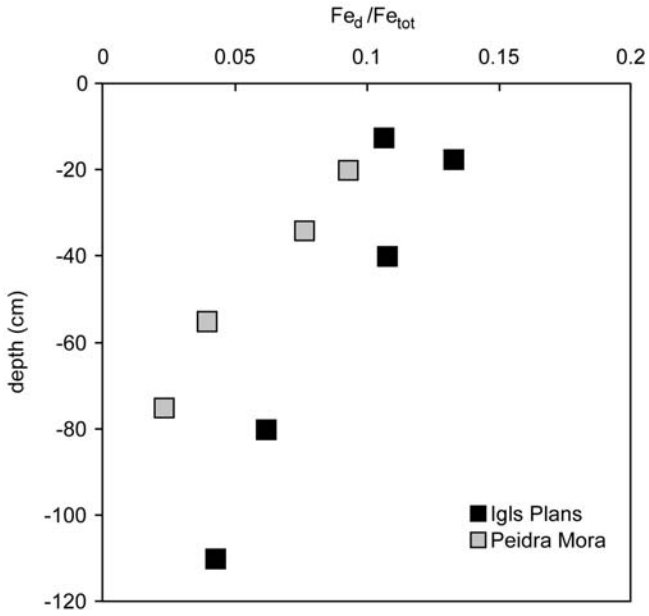

Fig. (10). Fe_d/Fe_{tot} ratio as a weatheirng indicator along the soil profiles (d = dithionite-extractable fraction, tot = total content).

DISCUSSION

Frauenfelder *et al*. [2] and Laustela *et al*. [11] measured Schmidt-hammer rebound values that varied from approx. 40-45 near the rock glacier tongue (Holocene aged) to 50–55 in the root zone (present day situation) on a number of active rock glaciers with a comparable lithology near our investigation area. Additionally, Böhlert *et al*. [63] have shown that Lateglacial features (moraines, rock glaciers; Pre- and Post-Egesen) have rebound values usually between 30 and 40 and that values on active rock glaciers (covering the Holocene) normally range between 40 and 55, depending on the position of the measured transect. Our measured values on present-day active rock glaciers correspond well to above values. The median as well as the modal values of weathering rind measurements [11] are equally suitable to delineate the increasing weathering rind thicknesses with the duration of exposure. The good correlation between the weathering rind data and the Schmidt-hammer rebound values (Fig. **11**) additionally demonstrates the potential of a combined method application in Alpine rock glaciers areas. Based on the Schmidt-hammer and weathering rind measurements, the relict rock glacier Alvra can be seen as another, older rock glacier generation than the present-day active ones. Both methods clearly show that the rock glacier Alvra was exposed to weathering processes earlier than the others. Weathering rind thicknesses most clearly reflect the polymorphic character of this rock glacier. Similar to Birkeland [64] where deposits of the Pinedale glaciation (≥ 10 kyr) could be discerned from younger Neoglacial moraines (3 – 5 kyr), weathering rinds provide a good weathering index for relative age assignment.

Mass balance calculations have indicated that extensive mineral weathering here has resulted in significant leaching losses of Al, Fe and Si particularly from upper soil horizons. The soil "Igls Plans" is more weathered than soil "Peidra Mora" and shows relative element losses that are close to

Table 3. Cosmogenic Nuclide Concentrations and Calculated Exposure Ages for the Albula-Region. Ages were Calculated Using an Erosion Rate of 3 mm per 1000 Years. To Emphasize the Influence of Erosion and Snow Coverage, Values without Correction (A) are Shown as Well as Ages with Two Different Estimated Snow Heights, in Each Case Only for Snow (B, D) and Additionally for Erosion (C, E)

Location	**Roche Moutonnée Crap Alv**	
Sample codes	**Alb 7**	**Alb 8**
Latitude (°N)	46.58	46.58
Longitude (°E)	9.80	9.80
Elevation (m a.s.l.)	2060	2070
Sample material	Granite	Granite
Sample thickness (cm)	4.5	3.5
Quartz (g)	56.45	56.49
^{10}Be (atoms $g^{-1}*10^4$)	28.23	27.06
Surface dip angle (°)	10	20
Dip direction	50	85
Measurement error (%)	5.0	12.0
Local production rate (atoms g^{-1} yr^{-1})	26.87	27.06
Production rate (atoms g^{-1} yr^{-1}) *	25.28	25.61
Correction factor for shielding	0.977	0.975
(A) ^{10}Be date (yrs) (uncorrected) **	**11200 ± 760**	**10590 ± 1390**
Estimated snow cover (m for 6 months yr^{-1})	0.8	0.8
(B) ^{10}Be date (yrs) (Corrected for snow) **	**12090 ± 820**	**11440 ± 1490**
(C) ^{10}Be date (yrs) (Corrected for erosion and snow) **	**12480 ± 850**	**11780 ± 1530**
Estimated snow cover (m for 6 months yr^{-1})	1.0	1.0
(D) ^{10}Be date (yrs) (Corrected for snow) **	**12320 ± 840**	**11660 ± 1510**
(E) ^{10}Be date (yrs) (Corrected for erosion and snow) **	**12720 ± 860**	**12020 ± 1560**

*Production rate corrected for shielding (atoms g^{-1} yr^{-1}).
** Estimated total error including measurement error and the effects of altitude, latitude scaling, topography, depth.

soils that developed over post-Egesen time [60, 61, 64, 65]. The soil "Peidra Mora" shows typical weathering rates of a soil that must have an age of < 10 ky [60, 61]. This is in agreement with the age determinations of the stable soil organic matter.

Table 4. Radiocarbon Dating of the Stable Soil Organic Matter of the Site Peidra Mora. Calibrated ^{14}C Ages are Given in the 2-σ Range

Horizon	**Depth [cm]**	**Sample Number**	**^{14}C Age (y BP)**	**δ^{13}C (%)**	**^{14}C Age (cal yBP; Oxcal 4.1)**
OE	13-27	UZ-5655	3630 ± 50	-20.1 ± 1.1	4139 – 3832
Bs	27-40	UZ-5656	5135 ± 50	-19.5 ± 1.1	5992 – 5748

Although some uncertainties still exist about the timing of rock glacier activities, two distinct phases of rock glacier activity could be discerned. This finding was only made possible using a multi-parameter approach that consequently clearly shows its advantages [66, 67].

Active rock glaciers creep as long as they remain within areas with permafrost conditions [68, 69]. Today's relict rock glaciers document the local lower limit of permafrost at the time of their decay where flow is not restricted to topography [70]. Frauenfelder *et al.* [70] estimated the differences in mean annual air temperature between the Younger Dryas period and today using the topographic position of 32 relict rock glaciers in the Err-Julier area (Swiss Alps) and, therefore, close to the Albula region. Their results suggest that mean annual air temperature during the Younger Dryas was c. 3 - 4 °C lower than modern values ($\Delta T = T_p - T_f$; with T_p = present day mean annual temperature and T_f = former mean annual temperature) and that the lower limit of permafrost was depressed considerably more than the glacier equilibrium lines. This indicates remarkably drier conditions than today. The present-day limit of permafrost at north-facing sites varies in our investigation area (Albula region) in the range 2400 to 2600 m asl (see Fig. **4**; rock glaciers A – D) depending on the topography. The front of rock glacier E is at 2040 m asl. The local lapse rate is near 0.55 °C/100m [70]. For rock glacier E, ΔT would be roughly between 2 °C and 3.1 °C. This clearly suggests an advance of this rock glacier in the Younger Dryas. The calculation coincides with those of [70] who suggested that permafrost had been present in areas above c. 1950 m asl in slopes exposed to north, above 2200 m asl in easterly exposed areas, above 2450 m asl on south-

faced slopes and above 2150 m asl in west-exposed slopes (i.e. 500m to 600m below the present-day limits if discontinuous permafrost). According to [70], relict rock glaciers with ΔT around 3°C were probably active during the Younger Dryas and presumably disintegrated by the end of the transition from the Alpine Lateglacial to the Holocene [70].

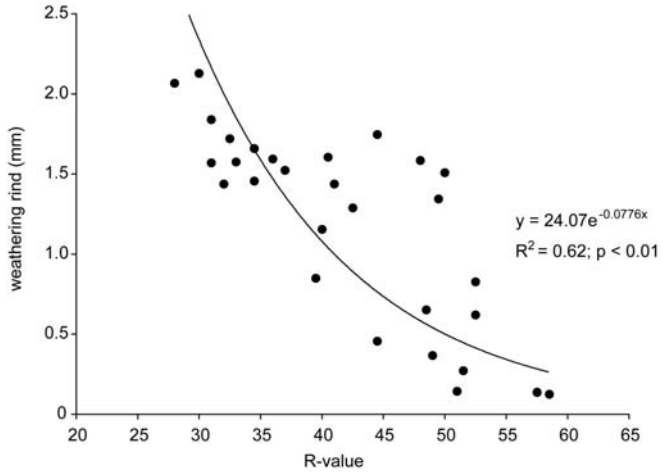

Fig. (11). Comparison between the Schmidt-hammer rebound values (mean value) and the weathering rind thickness (mean values).

The surface exposure and peat bog dating, and the weathering status of the soil "Igls Plans" provide a minimum-limiting age estimate for the earliest start of rock glacier activity (Alvra; see Fig. **12**). The relict rock glacier Alvra (E) started its activity during the waning stages of the Egesen (see also above). We hypothesise that this activity most probably continued also in the Holocene, at most until to the climatic optimum (9 – 5 ky BP; between the Boreal and the Older Atlanticum chronozones; [71]). The start of the activity of the present-day active rock glaciers (rock glaciers A – D) cannot be precisely determined. Rock glaciers typically show a "caterpillar-like" flow behaviour: boulders at the surface fall down at the oversteepened front and are subsequently overridden by the ice-supersaturated fine material. This results in an age inversion, i.e. at the surface the blocks are increasingly older towards the rock glacier front, for the boulder bottom layer the opposite is true [68]. Dating of rock material near the front thus always provides minimum ages, as the oldest material is inaccessible under the rock glacier body. However, they most probably started their activity not much before the onset of the Holocene or Holocene climatic optimum. It is probable that little remnants of local glaciers still existed in the shadowy parts of the north exposed slope which hindered the development of creeping permafrost structures. We assume that these local glaciers completely melted no later than the climate optimum which then gave rise to an increased production of debris and consequently to the

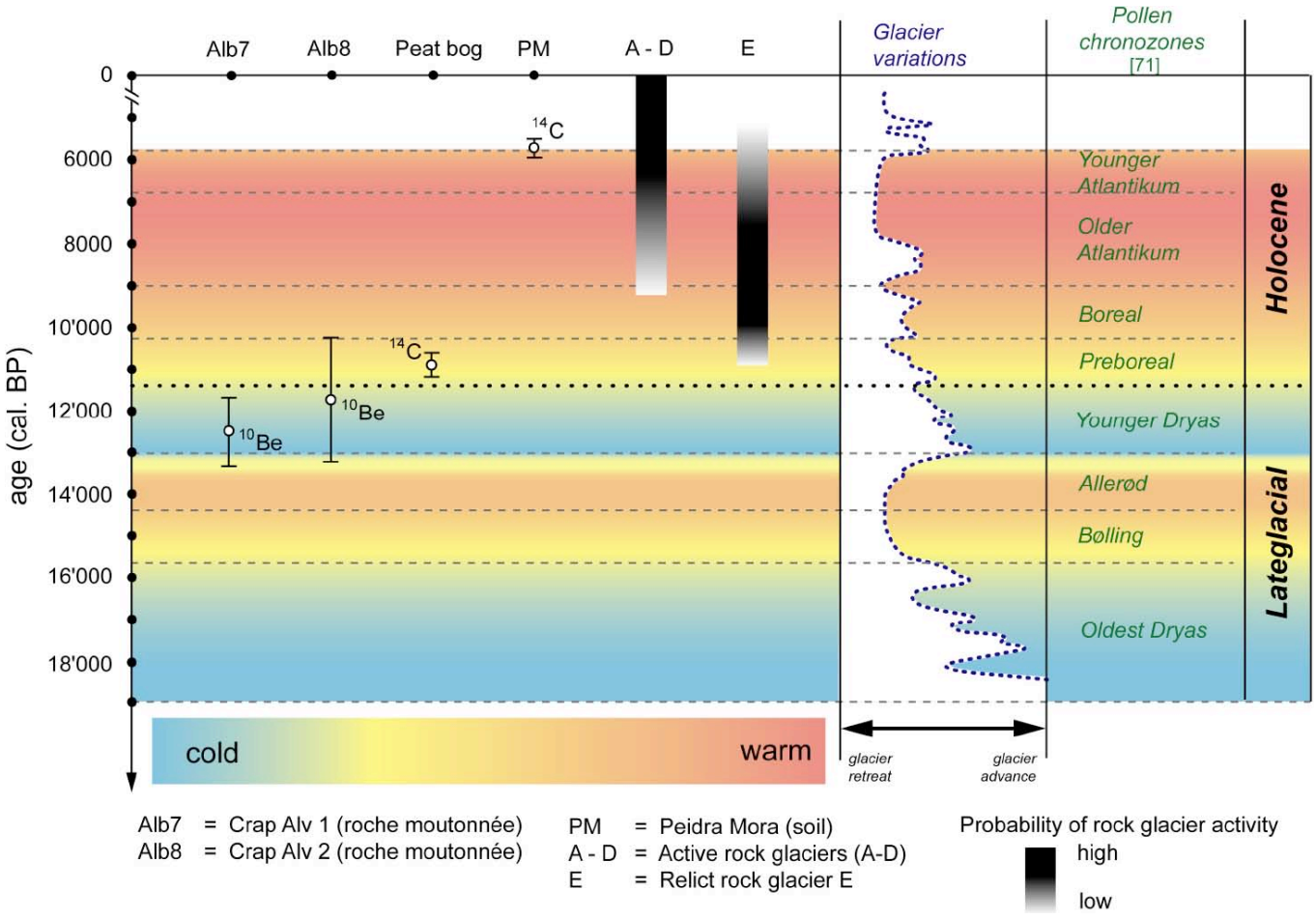

Fig. (12). Time marks (calibrated time scale) and hypothesised duration of rock glacier activity in the investigation area.

formation of rock glaciers. Consequently, two main phases of rock glacier activity could be derived: one starting immediately after the retreat of glaciers during the Younger Dryas (Egesen glacial states) and the other one during the Holocene. The start of the second phase cannot be determined precisely but should have started c. 10 - 6ky BP.

CONCLUSIONS

In this study we attempt to identify phases of rock glacier activity in a high Alpine environment of the Swiss Alps using a multi-parameter approach to age analysis. We obtained the following main findings:

- A distinct increase in weathering rind thickness and decrease of the Schmidt hammer rebound values along the rock glaciers (i.e. with increasing age) could be measured. Both methods reflect equally well the effect of weathering with increasing age.
- Surface exposure dating (SED) of a roche moutonnée using ^{10}Be, ^{14}C dating of a peat bog, the palynological investigations as well as glaciomorphologic mapping [25] delimited the maximum age of the Lateglacial permafrost activity. SED, ^{14}C and glaciomorphologic mapping data suggest an earliest start of permafrost activity shortly after the Younger Dryas (11.6 ky). Palynological investigations show that these activities must be certainly younger than the pre-Allerød (Allerød: 14.7 – 12.9 ky BP).
- Soil analyses confirmed and added an additional time constraint. The older soil, in front of the relict rock glacier, was highly weathered and must have started its evolution in the Lateglacial (shortly after the Younger Dryas). The younger soil, which can be considered to constrain the age of the active rock glaciers, started forming about 6ky BP.
- As a result, two main phases of rock glacier activity could be derived: one starting immediately after the retreat of glaciers during the Younger Dryas (Egesen glacial states; rock glacier E) and the other one in the Holocene (rock glaciers A – D). The start of the second phase could not be determined precisely but should have started c. 10 - 6ky BP.
- The strategy of a combined application of relative and numerical dating techniques is promising. This leads to additional datasets, provides the ability to cross-check each of the methods and to revise previous interpretations.

ACKNOWLEDGEMENTS

We would like to express our appreciation to B. Kägi for his assistance in the laboratory. This study was supported by the Swiss National Science Foundation grant number 20-109565/1. We are, furthermore, indebted to Aldo Mirabella, Dennis Dahms and an unknown reviewer for their helpful comments on an earlier version of the manuscript.

REFERENCES

[1] Haeberli W, Hallet B, Arenson L, *et al*. Permafrost creep and rock glacier dynamics. Permafr Perigla Proc 2006; 17: 189-214.

[2] Frauenfelder R, Laustela M, Kaeaeb A. Relative age dating of Alpine rockglacier surfaces. Ann Geomorphol 2005; 49: 145-66.

[3] Ballantyne CK, Schnabel C, Xu S. Exposure dating and reinterpretation of coarse debris accumulations ('rock glaciers') in the Cairngorm Mountains, Scotland. J Quat Sci 2009; 24: 19-31.

[4] Chinn TJH. Use of rock weathering-rind thickness for Holocene absolute age-dating in New Zealand. Arct Alp Res 1981; 13: 33-45.

[5] Gellatly AF. The use of rock weathering-rind thickness to redate moraines in Mount Cook National Park, New Zealand. Arct Alp Res 1984; 16: 225-32.

[6] McSaveney MJ. A manual for weathering-rind dating of grey sandstones of the Torlesse Supergroup, New Zealand. Lower Hutt: Institute of Geological & Nuclear Sciences Limited 1992.

[7] Ricker KE, Chinn TJ, McSaveney MJ. A late Quaternary moraine sequence dated by rock weathering rinds, Craigieburn Range, New Zealand. Can J Earth Sci 1993; 30: 1861-9.

[8] Whitehouse IE, McSaneney MJ, Knuepfer PLK, Chinn TJH. Growth of Weathering Rinds on Torlesse Sandstone, Southern Alps, New Zealand: Academic Press 1986: pp. 419-35.

[9] Colman SM, Pierce KL. Correlation of Quaternary glacial sequences in the western United States based on weathering rinds and related studies. In: Mahaney WC, Ed. Correlation of Quaternary chronologies. Norwich, England: Geobooks: 1985; pp. 437-53.

[10] Oguchi CT. A porosity-related diffusion model of weathering-rind development. Catena 2004; 58: 65-75.

[11] Laustela M, Egli M, Frauenfelder R, Haeberli W. Weathering rind measurements and relative age dating of rock-glacier surfaces in crystalline regions of the Swiss Alps. In: Phillips M, Springman SM, Arenson LU, Eds. Proceedings of the eighth international conference on permafrost (ICOP 2003). A. A. Balkema Publishers, Lisse 2003; Vol. I: pp. 627-32.

[12] Pelt E, Chabaux F, Innocent C, Navarre-Sitchler AK, Sak PB, Brantley SL. Uranium–thorium chronometry of weathering rinds: rock alteration rate and paleo-isotopic record of weathering fluids. Earth Planet Sci Lett 2008; 276: 98-105.

[13] Kaufmann V. Deformation analysis of the Doesen rockglacier (Austrian Alps, Europe). In Lewkowicz AG, Allard M, Eds. 7th International Conference on Permafrost (Yellowknife, 23-27 June 1998), Collection Nordicana 57. Centre d'Etudes Nordiques, Université Laval, Québec 1998; pp. 551-6.

[14] Winkler S, Shakesby RA. Anwendung von Lichenometrie und Schmidt-Hammer zur relativen Altersdatierung prä-frührezenter Moränen am Beispiel der Vorfelder von Guslar-, Mitterkar-, Rofenkar- und Vernagtferner (Ötztaler Alpen/Österreich). Petermanns Geographische Mitteilungen 1995; 139: 283-304.

[15] Haeberli W, Hoelzle M, Kääb A, Keller F, Vonder Mühll D, Wagner S. Ten years after drilling through the permafrost of the active rock glacier Murtèl, eastern Swiss Alps: answered questions and new perspectives. In: Lewkowicz AG, Allard M, Eds. 7th International Conference on Permafrost (Yellowknife, 23-27 June 1998), Collection Nordicana 57, Centre d'Etudes Nordiques, Université Laval, Québec 1998: pp. 403-10.

[16] Kääb A, Haeberli W, Gudmundsson GH. Analysing the creep of mountain permafrost using high precision aerial photogrammetry: 25 years of monitoring Gruben rockglacier, Swiss Alps. Permafr Perigl Proc 1997; 8: 409-26.

[17] Haeberli W, Brandova D, Castelli S, *et al*. Methods for absolute and relative age dating of rock-glacier surfaces in alpine permafrost. In: Phillips M, Springman SM, Arenson LU, Eds. Proceedings of the eighth international conference on permafrost (ICOP 2003), A. A. Balkema Publishers: Lisse, 2003; Vol. I: pp. 343-48.

[18] Cornelius HP. Geologische Karte der Err-Julier-Gruppe, Bern, Spezialkarte Nr. 115, 1929.

[19] Cornelius HP. Geologie der Err-Julier-Gruppe. Beiträge zur Geologischen Karte der Schweiz, Bern, N.F., 70. Lief., 1. Teil (Das Baumaterial), 1935.

[20] Bearth P, Heierli H, Roesli F. Geologischer Atlas der Schweiz, Blatt 1237 Albulapass (Atlasblatt 81). Schweizerische Geologische Kommission und Landeshydrologie und –geologie, Bern1987.

[21] Schwarb M, Daly C, Frei C, Schär C. Mittlere jährliche Niederschlagshöhe im europäischen Alpenraum 1971-1990. Hydrologischer Atlas der Schweiz, Blatt 2.6., Bern 2000.

[22] Jäckli H. Die Schweiz zur letzten Eiszeit. Atlas der Schweiz, map 6, Wabern-Bern, Eidg. Landestopographie 1970.

[23] Ivy-Ochs S, Kerschner H, Reuther A, *et al*. The timing of glacier advances in the northern European Alps based on surface exposure dating with cosmogenic ^{10}Be, ^{26}Al, ^{36}Cl, and ^{21}Ne. In: Siame LL, Bourles DL, Brown ET, Eds. In Situ Cosmogenic Nuclides and their Applications in Earth Sciences. Geol Soc Am Special Paper 2006; 415: 43-60.

[24] Florineth D, Schlüchter S. Alpine evidence for atmospheric circulation patterns in Europe during the Last Glacial Maximum. Quat Res 2000; 54: 295-308.

[25] Maisch M. Glazialmorphologische und gletschergeschichtliche Untersuchungen im Gebiet zwischen Landwasser- und Albulatal (Kt. Graubünden, Schweiz). PhD thesis, University of Zurich, Switzerland 1981.

[26] Coaz J. Topographischer Atlas der Schweiz, Blatt Bevers. Schweiz. Eidg. Stabsbureau, Bern 1878.

[27] FOEN (Federal Office for the Environment). Hinweiskarte der potentiellen Permafrostverbreitung in der Schweiz, Blatt Bergün 2005. Map of the potential permafrost distribution of Switzerland, map sheet Bergün 2005.

[28] Schmidt E. A Non-destructive concrete tester. Concrete 1951; 59: 34-35.

[29] Matthews JA, Shakesby RA. The status of the "Little Ice Age" in Southern Norway; relative age dating of Neoglacial moraines with Schmidt hammer and lichenometry. Boreas 1984; 13: 333-46.

[30] Winkler S. The little ice age maximum in the Southern Alps, New Zealand: preliminary results at Mueller Glacier. Holocene 2000; 10: 643-7.

[31] Kellerer-Pirklbauer A, Wangensteen B, Farbrot H, Etzelmüller B. Relative surface age-dating of rock glacier systems near Hólar in Hjaltadalur, northern Iceland. J Quat Sci 2008; 23: 137-51.

[32] Nesje A, Blikra LH, Anda E. Dating rockfall-avalanche deposits from degree of rock-surface weathering by Schmidt-hammer tests: a study from Norangsdalen, Sunnmøre, Norway. Norwegian J Geol 1994; 74: 108-13.

[33] Engel Z. Measurement and age assignement of intact rock strength in the Krkonose Mountains, Czech Republic. Ann Geomorphol 2007; 51(Suppl. 1): 69-80.

[34] Shakesby RA, Matthews JA, Owen G. The Schmidt hammer as a relative-age dating tool and its potential for calibrated-age dating in Holocene glaciated environments. Quat Sci Rev 2006; 25: 2846-67.

[35] Day MJ, Goudie AS. Field assessment of rock hardness using the Schmidt hammer. British Geomorphological Research Group. Tech Bull 1977; 18: 19-29.

[36] Oguchi CT. Formation of weathering rinds on andesite. Earth Surf Proc Landf 2001; 26: 847-58.

[37] Gordon SJ, Dorn RI. In situ weathering rind erosion. Geomorphology 2005; 67: 97-113.

[38] Hossner CR. Dissolution for total elemental analysis. In: Sparks DL, Ed. Methods of Soil Analysis, Part 3 Chemical Methods. Madison, Wisconsin: Soil Science Society of America Inc. and American Society of Agronomy Inc. 1996: pp. 49-64.

[39] McKeague JA, Brydon JE, Miles NM. Differentiation of forms of extractable iron and aluminium in soils. Soil Sci Soc Am Proc 1971; 35: 33-8.

[40] Bascomb CL. Physical and chemical analyses of <2 mm samples. In: Avery BW, Bascomb CL, Eds. Soil Survey Laboratory Methods. Soil Survey Tech. Monog. 6; 1974: pp. 14-41.

[41] Plante AF, Chenu C, Balabane M, Mariotti A, Righi D. Peroxide oxidation of clay-associated organic matter in a cultivation chronosequence. Eur J Soil Sci 2004; 55: 471-8.

[42] Eusterhues K, Runpel C, Kögel-Knabner I. Stabilization of soil organic matter isolated *via* oxidative degradation. Org Geochem 2005; 36: 1567-75.

[43] Mikutta R, Kleber M, Torn MS, Jahn R. Stabilization of organic matter: association with minerals or chemical recalcitrance? Biogeochemistry 2006; 77: 25-56.

[44] Helfrich M, Flessa H, Mikutta R, Dreves A, Ludwig B. Comparison of chemical fractionations methods for isolating stable soil organic carbon pools. Eur J Soil Sci 2007; 58: 1316-29.

[45] Favilli F, Egli M, Cherubini P, Sartori G, Haeberli W, Delbos E. Comparison of different methods of obtaining a resilient organic matter fraction in Alpine soils. Geoderma 2008; 145: 355-69.

[46] Bronk RC. Development of the radiocarbon calibration program OxCal. Radiocarbon 2001; 43: 355-63.

[47] Reimer PJ, Baillie MGL, Bard E, *et al*. IntCal04 terrestrial radiocarbon age calibration, 0-26 cal kyr BP. Radiocarbon 2004; 46: 1029-58.

[48] Gosse JC, Phillips FM. Terrestrial in situ produced cosmogenic nuclides: Theory and application. Quat Sci Rev 2001; 20: 1475-560.

[49] Masarik L, Wieler R. Production rates of cosmogenic nuclides in boulders. Earth Planet Sci Lett 2003; 216: 201-8.

[50] Kohl CP, Nishiizumi K. Chemical isolation of quartz for measurement of in-situ produced cosmogenic nuclides. Geochim Cosmochim Acta 1992; 56: 3583-7.

[51] Ivy-Ochs S. The dating of rock surfaces using in situ produced ^{10}Be, ^{26}Al and ^{36}Cl, with examples from Antarctica and the Swiss Alps. PhD Thesis, No. 11763. ETH Zurich 1996.

[52] Stone JO. Air pressure and cosmogenic isotope production. J Geophys Res 2000; 105/B10: 753-9.

[53] Dunne J, Elmore D, Muzikar P. Scaling factors fot the rates of production of cosmogenic shielding and attenuation at depth on sloped surfaces. Geomorphology 1999; 27: 3-11.

[54] Auer M. Regionalisierung von Schneeparametern – Eine Methode zur Darstellung von Schneeparametern im Relief. Publikation Gewässerkunde 2003; p. 304.

[55] Soil Survey Staff. Keys to Soil Taxonomy, 11th ed. Washington, DC: USDA-Natural Resources Conservation Service 2010.

[56] Brimhall GH, Dietrich WE. Constitutive mass balance relations between chemical composition, volume, density, porosity, and strain in metasomatic hydrochemical systems: results on weathering and pedogenesis. Geochim Cosmochim Acta 1987; 51: 567-87.

[57] Chadwick OA, Brimhall GH, Hendricks DM. From a black to a gray box – a mass balance interpretation of pedogenesis. Geomorphology 1990; 3: 369-90.

[58] Egli M, Fitze P. Formulation of pedologic mass balance based on immobile elements: a revision. Soil Sci 2000; 165: 437-43.

[59] Brantley SL, Goldhaber MB, Ragnarsdottir KV. Crossing disciplines and scales to understand the critical zone. Elements 2007; 3: 307-14.

[60] Egli M, Mirabella A, Fitze P. Weathering and evolution of soils formed on granitic, glacial deposits: results from chronosequences of Swiss Alpine environments. Catena 2001a; 45: 19-47.

[61] Egli M, Mirabella A, Fitze P. Clay mineral formation in soils of two different chronosequences in the Swiss Alps. Geoderma 2001b; 104: 145-75.

[62] Cerling TE, Craig H. Geomorphology and in-situ cosmogenic isotopes. Annu Rev Earth Planet Sci 1994; 22: 273-317.

[63] Böhlert R, Egli M, Maisch M, *et al*. Application of a combination of dating techniques to reconstruct the Lateglacial and early Holocene landscape history of the Albula region (eastern Switzerland). Geomorphology 2010; doi:10.1016/j.geomorph.2010.10.034.

[64] Birkeland PW. Use of relative age-dating methods in a stratigraphic study of rock-glacier deposits, Mt. Sopris, Colorado. Arct Alp Res 1973; 5: 401-16.

[65] Egli M, Mirabella A, Fitze P. Formation rates of smectites derived from two Holocene chronosequences in the Swiss Alps. Geoderma 2003; 117: 81-98.

[66] Favilli F, Egli M, Brandová D, *et al*. Combined use of relative and absolute dating techniques for detecting signals of Alpine landscape evolution during the late Pleistocene and early Holocene. Geomorphology 2009; 112: 48-66.

[67] Birkeland PW, Burke RM, Shroba RR. Holocene alpine soils in gneissic cirque deposits, Colorado Front Range. U.S. Geol Survey Bull 1987; vol. 1590-E: 21.

[68] Haeberli W. Creep of mountain permafrost: internal structure and flow of Alpine rockglaciers. Mitteilungen der VAW ETH Zürich. 1985; 77: 142.

[69] Barsch D. Rockglaciers. Indicators for the Present and Former Geoecology in High Mountain Environments. Berlin: Springer Series in Physical Environment 16, Springer Verlag 1996.

[70] Frauenfelder R, Haeberli W, Hoelzle M, Maisch M. Using relict rockglaciers in GIS-based modelling to reconstruct Younger Dryas permafrost distribution patterns in the Err-Julier area, Swiss Alps. Norsk geogr Tidsskr 2001; 55: 195-202.

[71] Maisch M, Wipf A, Denneler B, Battaglia J, Benz C. Die Gletscher der Schweizer Alpen. Gletscherhochstand 1850, aktuelle Vergletscherung, Gletscherschwund- Szenarien. Schlussbericht NFP 31 Projekt, vdf-Hochschulverlag ETH Zürich 1999.

Received: December 10, 2009 Revised: October 18, 2010 Accepted: October 22, 2010